ECS Transactions, 57 (1) 2279-2288 (2013)
10.1149/05701.2279ecst ©The Electrochemical Society

Long Term Resistivity Behavior of SOFC Interconnect/Ni-mesh/Anode Interfaces

V. Sarda[a], S. Auvinen[b], V. Shemet[c], W. J. Quadakkers[c], M. Pihlatie[b], J. Kiviaho[b] and L. G. J. de Haart[a]

[a] Institute of Energy and Climate Research, Fundamental Electrochemistry (IEK-9), Forschungszentrum Jülich, 52425 Jülich, Germany
[b] VTT Technical Research Center of Finland, Espoo, Finland
[c] Institute of Energy and Climate Research, Microstructure and Properties of Materials (IEK-2), Forschungszentrum Jülich, 52425 Jülich, Germany

Contact resistances between Crofer 22 APU and Crofer 22 H interconnect plates, Ni mesh and Ni-8YSZ anode interfaces were measured under an anode gas atmosphere (97%H_2 + 3%H_2O) at 700 °C and 800 °C and current densities of 0 and 0.7 A/cm^2 for durations up to 3000 hours using the 4-point DC conductivity technique. Phase transformations within the steel samples close to the interface due to inter-diffusion of elements (Ni, Fe, Mn and Cr) were observed and analyzed. These phase transformations and the formation of oxide scales on steel as well as nickel mesh surface and grain boundaries do not seem to substantially affect the measured contact resistance with time.

Introduction

To ensure long term stable operation of Solid Oxide Fuel Cells (SOFC), details of the degradation mechanisms that occur during continuous (baseline) operation need to be understood. This should help in developing models that can predict the degradation phenomena and their combined effect on SOFC cells and single repeating units. This formulates the goal of the European SOFC-Life project (1). As part of Work Task 1.3 of the SOFC-Life project, SOFC anode degradation effects are analyzed with the help of single elements cut out of the anode compartment and whose degradation is governed by a single effect. This allows the separation of degradation mechanisms and helps in studying their dependencies on current, temperature, fuel type and water vapor content. Hence an attempt is made to obtain the evaluation and quantification of,

- The structural change in nickel cermet anodes, and
- The influence of diffusion phenomena between anode, anode contacting and anode side interconnect on contact resistance

Previous studies (2) have observed the migration of Nickel from anode and/or contact-mesh into the steel and the metal from the steel into the nickel resulting in the conversion of ferrite to austenite in the interconnect steel and in the corrosion of nickel. The coefficients of thermal expansion for austenite and ferrite substantially differ; with 18×10^{-6} K^{-1} (20 °C – 800 °C), austenite has a significantly higher coefficient of thermal expansion than ferrite (11.8×10^{-6} K^{-1}) (3), and thermal cycling may cause cracking and loss of contact (points). In this project, the focus lies on long term performance, hence transient effects caused from cycling are excluded. As far as known to the authors, the

Downloaded on 2014-01-13 to IP 134.94.122.141 address. Redistribution subject to ECS license or copyright; see ecsdl.org/site/terms_use

influence of these phenomena on the electrochemical performance of the SOFC in terms of the Area Specific Resistance (ASR) from varying temperature, current flow etc. have not been investigated so far. Experimental work in this paper intends to concentrate on these issues.

Experimental

Sample Scheme

Inter-diffusion tests are initially performed with a single Ni mesh and steel plate to understand the long term behavior in a simulated anode gas atmosphere (Ar + 4%H_2 + 2%H_2O) at 800 °C up to 3000 h. Samples of interconnect steel materials Crofer 22 APU and Crofer 22 H, whose compositions are shown in Table 1, were in the dimensions of 20x50x1 mm^3. The contact between the Ni-mesh and steel was accomplished by spot-welding.

TABLE I. Elemental composition of the supplied Crofer 22 APU and Crofer 22 H in wt %, Fe balance and S<0.002

Interconnect Steel Type	Cr	C	N	Mn	Si	Al	W	Nb	Ti	La
Crofer22APU	23	0.004	0.004	0.45	< 0.05	< 0.05	-	-	0.06	0.1
Crofer22H	23	0.007	0.02	0.45	0.25	< 0.05	2	0.5	0.06	0.1

The above tests are followed by 4 probe DC Conductivity measurements to obtain the long term resistivity of the Ni mesh, steel and anode substrate interfaces. For this test, platinum wires (0.5 mm in diameter) were spot welded to the steel plates (dimensions of 20x20x1 mm^3) as potential probes and current contacts. Ni-mesh was spot-welded (at 4 spots) to one surface of the steel plates. In all samples one Ni wire was left extending approximately 2 cm out of the mesh as an extra potential probe. The NiO-YSZ anode substrate (19.5x19.5 mm^2) is 500 µm thick including the supplied anode functional layer which is around 5 µm thick. Hence, in these experiments sandwiches were made which included the anode substrate placed between the steel plates welded to the Ni mesh on one surface as shown in Figure 1. Ceramic and metal blocks were used as weights for the sandwich samples to ensure a contact pressure of 5 $N.cm^{-2}$. All steel samples were polished to a 1200 grit finish. Ni-mesh with a thickness of 130 µm and mesh number 150 was used.

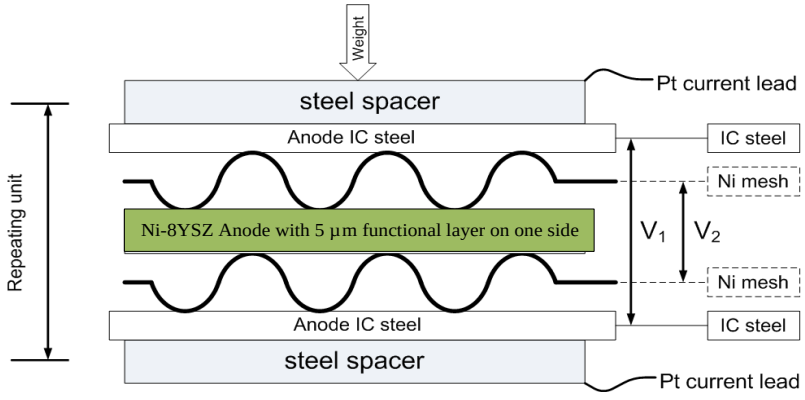

Figure 1. The assembly of a single sandwich of tested materials including steel, Ni mesh and anode cermet and the measured potential differences.

Downloaded on 2014-01-13 to IP 134.94.122.141 address. Redistribution subject to ECS license or copyright; see ecsdl.org/site/terms_use

Hence the single repeating unit consisted of sandwiches of Crofer22APU – Ni mesh – NiO/YSZ cermet – Ni mesh – Crofer 22 APU and Crofer 22 H – Ni mesh – NiO/YSZ cermet – Ni mesh – Crofer 22 H and the designation of the potential contacts that were measured is shown in Figure 1.

Setup and Procedure

The tests are conducted in a vertical Nabertherm three-zone furnace and the samples are fed with current by a Delta Elektronica PSU ES 030-10. The potential signals from the samples are measured by an Agilent data acquisition unit 34970A with a multiplexer 34901A. An oxygen sensor has been positioned in the furnace to measure the partial pressure of oxygen during the heating up phase, reduction, measurement phase and cooling down.

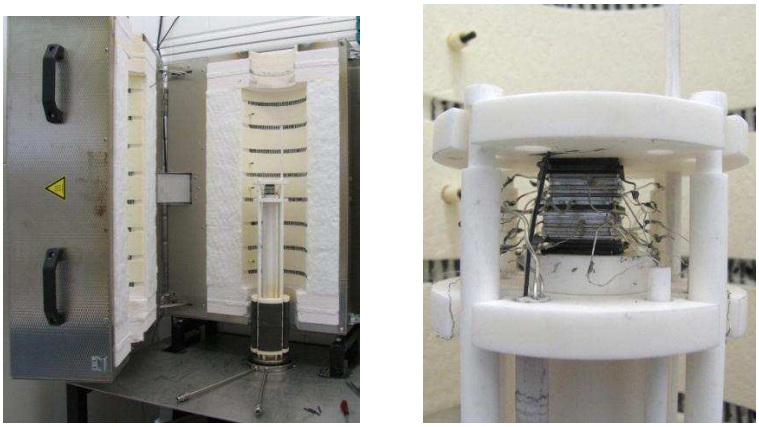

Figure 2. The furnace and the assembly of the samples inside.

Heating was carried out under a reducing atmosphere to avoid any pre-oxidation of the samples, i.e. 95%N_2 and 5%H_2 with a ramp rate of 1 °C/min up to the final temperature of 900 °C at which reduction is performed for the NiO-YSZ cermets. After a period of 75 minutes, the final gas composition consists of 97%H_2 with 3%H_2O. With this gas composition during heating the equilibrium oxygen partial pressure is $1.8 * 10^{-43}$ atm at 350 °C and $8.8 * 10^{-24}$ atm at 790 °C. When the measurements were recorded, the partial pressure of oxygen in the test chamber had been approximately 10^{-22} atm at 800 °C and 10^{-24} atm at 700 °C. Each sandwich sample type is either exposed to no current or a continuous current density of 0.7 $A.cm^{-2}$. The potential drop was measured separately for the two steel-Ni mesh interfaces and across the two Ni-mesh-anode interfaces. Current-Voltage (IV) measurements are conducted in the beginning of the test and every 330 h both at the operating temperature of 800 °C and at the reference temperature of 700 °C. The temperature in the furnace is always allowed to stabilize for a period of 15 minutes before the resistance measurements were carried out. The voltage is measured with current density values from -1 to 1 $A.cm^{-2}$. Linear regression is fitted to the IV plots to obtain the area specific resistance (ASR) in $m\Omega.cm^2$. After 3000 hours, the last reference measurement at 700 °C is obtained and the samples are cooled down to room temperature under 95%N_2 + 5%H_2. Subsequently, the sandwich samples are cut, ground, polished and analyzed by SEM+EDX to characterize the interfaces.

Downloaded on 2014-01-13 to IP 134.94.122.141 address. Redistribution subject to ECS license or copyright; see ecsdl.org/site/terms_use

Results and Discussion

Inter-diffusion Tests in Ar + 4%H_2 + 2%H_2O at 800 °C

The interface between the Ni-mesh and the tested steels and the corresponding elemental profiles after 1000 h are shown in Figure 3 and 4. SEM/EDX analyses showed that during long term exposure austenite grains form in the steel adjacent to the contact area. The austenitization may result in a reduction of the Cr diffusion in the steel, which may affect selective oxidation of Cr in the interconnect steel leading to poor oxidation resistance (4). The austenite layers have a width of approximately 40 µm and 50 µm for Crofer 22 H and Crofer 22 APU, respectively.

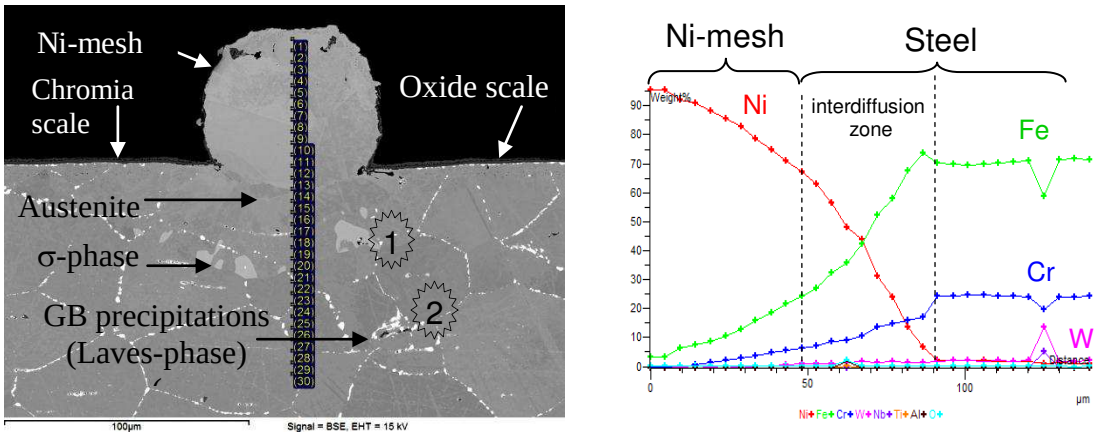

(a) (b)

Figure 3. SEM cross-section (a) and the corresponding distribution of the elements in terms of %weight expressed as function of the interfacial distance selected (b) in contact area between Ni-mesh and Crofer 22 H after 1000h test in Ar + 4%H_2 + 2%H_2O at 800 °C.

The EDX analyses revealed that Ni diffuses from the wire-mesh into the steel whereas Fe, Cr and Mn diffuse from the steel into the Ni-mesh. The latter leads to the formation of chromium and manganese oxides at the grain boundaries in the Ni-mesh while the diffusion of nickel into the ferritic steel results in the formation of austenite and σ-phase near the contact area (Figure 3a and Table 2). The disadvantage associated with the formation of a σ-phase is the tendency of the steel to embrittle (5). In the case of the Crofer 22 H, the σ-phase forms beneath the austenitic grains. The SEM/EDX analyses did not detect the σ-phase formation near the Ni-mesh contact with the ferritic steel Crofer 22 APU (Figure 4).

TABLE II. Chemical compositions in at.-% (determined by EDX) of analysis areas indicated in Figure 3a

Spectrum	Cr	Fe	Ni	Nb	W	Phase
1	35.9	58.7	2.6	0.0	2.9	σ-phase
2	13.7	49.7	2.5	17.6	16.5	Laves-phase

Figures 3b and 4b also show diffusion profiles for Cr, Ni, Fe and W in the area where Ni was in direct contact with Crofer 22 H and Crofer 22 APU, respectively. The profiles show that nickel diffuses faster in Crofer22APU than in Crofer22H. Besides, SEM/EDX

Downloaded on 2014-01-13 to IP 134.94.122.141 address. Redistribution subject to ECS license or copyright; see ecsdl.org/site/terms_use

analyses did not detect the Laves-phase on the austenite grains or near the Ni-mesh contact with Crofer 22 H. It is apparent that the Cr and Fe-profiles in the inter-diffusion zone shown in Figure 4b are flat and exhibit a constant concentration near the boundary with the ferritic matrix, but small amounts of nickel are also dissolved in the ferritic matrix near the austenitic grains. The shape of the Cr and Fe profiles obviously depends on the detailed chemical composition of the ferritic steel (Figures 3b and 4b).

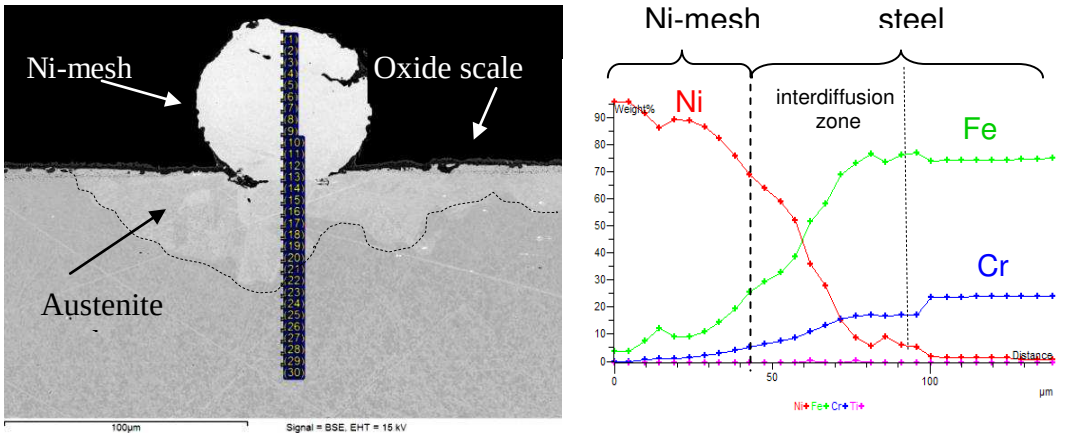

(a) (b)

Figure 4. SEM cross-section (a) and the corresponding distribution of the elements in terms of %weight expressed as function of the interfacial distance selected (b) in contact area between Ni-mesh and Crofer 22 APU after 1000 h test in Ar + 4%H_2 + 2%H_2O at 800 °C.

Longer exposure up to 3000 h of steel/nickel samples results in formation of a continuous austenite layer in the steel adjacent to the contact area (Figures 5a and 6a). Also, the chromium oxidizes as grain boundary oxide precipitates in the Ni-mesh. Thus, in the contact area between wire mesh and steel substantial changes of the mechanical properties of steel and nickel wire mesh may occur.

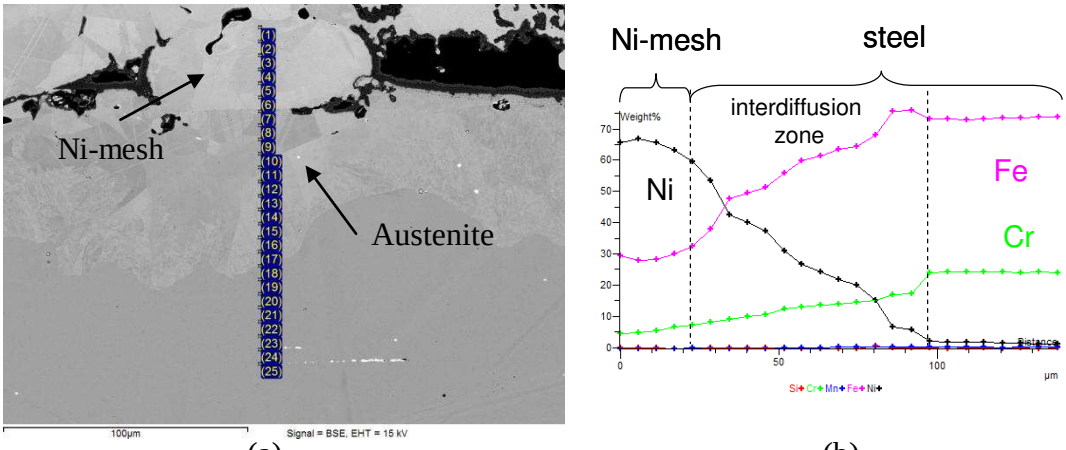

(a) (b)

Figure 5. SEM cross-section (a) and the corresponding distribution of the elements in terms of %weight expressed as function of the interfacial distance selected (b) in electrical contacts between Ni-mesh and Crofer 22 APU after 3000 h test in Ar + 4%H_2 + 2%H_2O at 800 °C.

Downloaded on 2014-01-13 to IP 134.94.122.141 address. Redistribution subject to ECS license or copyright; see ecsdl.org/site/terms_use

SEM/EDX analysis showed that more iron than chromium dissolved in the Ni-mesh. The iron concentration reaches more than 20 wt.-% in the nickel, but the chromium concentration reaches a value of only 5-7 wt.-% after 3000 h exposure. The uptake of chromium has as result that a chromia scale forms on the Ni-mesh after long term exposure in Ar+H_2/H_2O.

Important to note that SEM/EDX analyses did not detect presence of σ-phase near the Ni-mesh contact with both steel batches after 3000 h exposure (Figure 5a, 6a). From the diffusion profiles (Figures 5b, 6b), it can also be observed that the inter-diffusion zone is much larger, approximately 80 μm for the Crofer 22 APU, whereas for the Crofer 22 H it remains at almost the same depth as after 1000 hours.

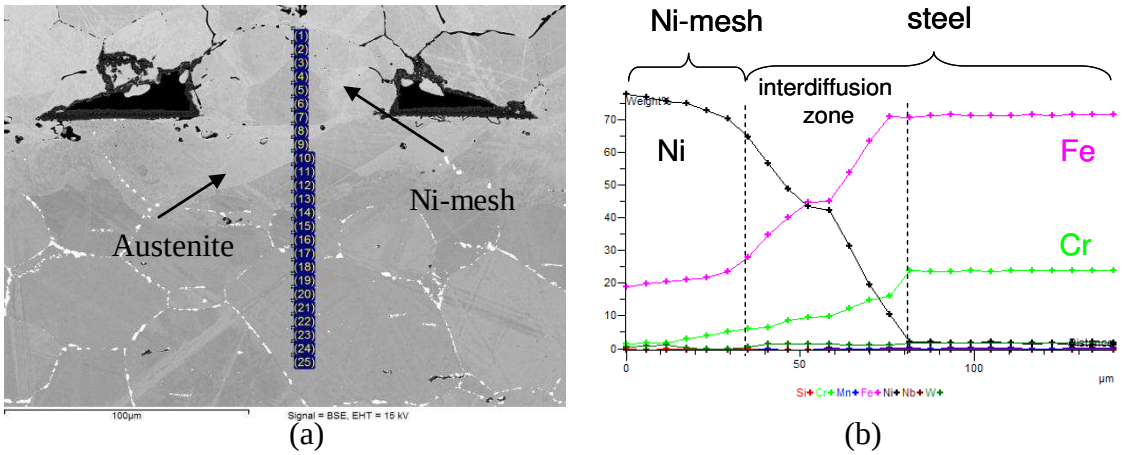

(a) (b)

Figure 6. SEM cross-section (a) and the corresponding distribution of the elements in terms of %weight expressed as function of the interfacial distance selected (b) in contact area between Ni-mesh and Crofer 22 H after 3000 h test in Ar + 4%H_2 + 2%H_2O at 800 °C.

Figure 7 shows kinetics of Ni-diffusion into the two tested ferritic steels at 800 °C. It can be observed that after 1000 hours, the difference in the depth up to which Ni diffuses into the Crofer 22 APU becomes substantial. Resistivity measurements are hence followed to investigate if this difference in diffusion of nickel and/or the formation of oxide layers contribute to the overall electrical performance in terms of the contact resistances.

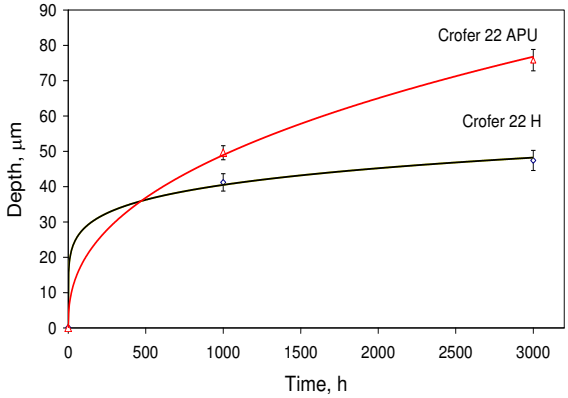

Figure 7. Depth of Ni-diffusion in ferritic steels in Ar-H_2-H_2O at 800°C as function of time.

Downloaded on 2014-01-13 to IP 134.94.122.141 address. Redistribution subject to ECS license or copyright; see ecsdl.org/site/terms_use

Resistivity Tests in 97%H_2 + 3%H_2O

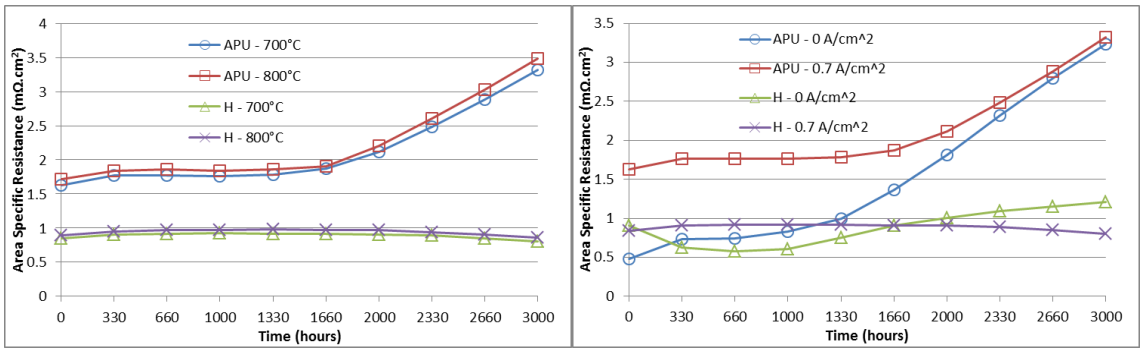

(a) (b)

Figure 8. Area Specific Resistance (ASR) as function of exposure time at 800 °C for Steel+Ni mesh+Ni-YSZ Cermet+Ni mesh+Steel sandwiches, (a) Comparison between ASR measured at 700 °C and 800 °C for the same sandwich sample subjected to constant current density of 0.7 A.cm^{-2} for 3000 h and (b) Comparison between ASR measured at constant temperature of 800 °C for two sandwich samples subjected to current density of 0 A.cm^{-2} and 0.7 A.cm^{-2} for 3000 h.

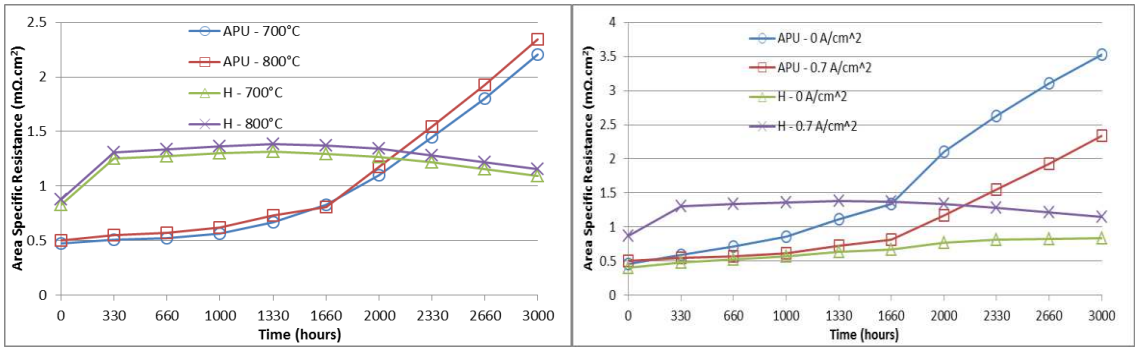

(a) (b)

Figure 9. Area Specific Resistance (ASR) as function of exposure time at 800 °C for Ni mesh+Ni-YSZ Cermet+Ni mesh sandwiches, (a) Comparison between ASR measured at 700 °C and 800 °C for the same sandwich sample subjected to constant current density of 0.7 A.cm^{-2} for 3000 h and (b) Comparison between ASR measured at constant temperature of 800 °C for two sandwich samples subjected to current density of 0 A.cm^{-2} and 0.7 A.cm^{-2} for 3000 h.

From Figures 8 and 9, it can be observed that the contacts with Crofer 22 APU steel and cermet exhibit a notable rise in the contact resistance whereas the rise in ASR with the Crofer 22 H and cermet contact is moderate at the end of the 3000 hours exposure. This same behavior can be seen in samples tested both with and without applied current (Figures 8b and 9b). The absolute increase in the ASR of both the steel types is higher for sandwich samples without than with an applied current density of 0.7 A.cm^{-2}. All samples show a slight increase in ASR when heating from 700 °C to 800 °C at the same time point throughout the duration of the test, i.e. from 0 to 3000 hours (Figures 8a and 9a). It is also to be noted that this increase in ASR at 800 °C is observed when the potential drops V_1 (including the steel plate) and V_2 (excluding the steel plate) are measured for the same sandwich sample (Refer to Figure 1). Hence it can be stated that there exists

Downloaded on 2014-01-13 to IP 134.94.122.141 address. Redistribution subject to ECS license or copyright; see ecsdl.org/site/terms_use

metallic contact across both types of interfacial regions (Steel-Ni mesh and Ni mesh-Anode).

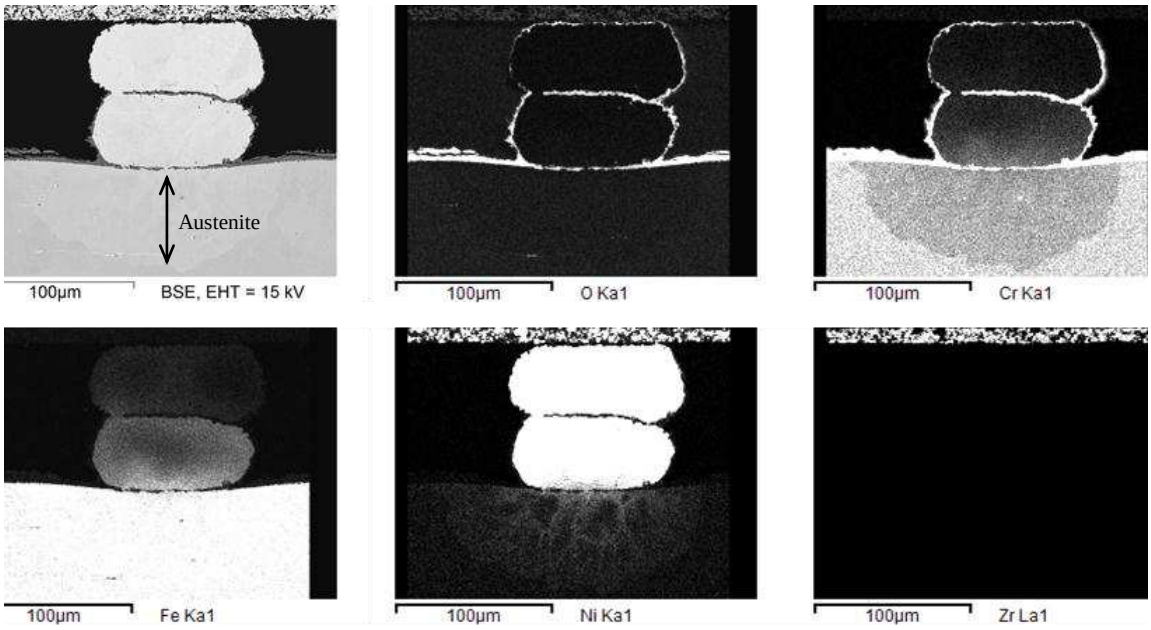

Figure 10. SEM image (upper left) and x-ray element mappings of the interfacial cross sections after 3000 hours of Crofer 22 APU Steel, Ni-YSZ Cermet and Ni mesh sandwich without applied current density. Respective elements and x-ray lines used (Kα or Lα) are indicated beneath the figures.

Similar to what was observed in the inter-diffusion tests; the SEM images and x-ray mappings from Figures 10 and 11 demonstrate diffusion of Cr, Mn and Fe into the Ni mesh and the diffusion of Ni into the steel at the Steel-Ni mesh contact interface. In addition, the depth of the austenitic region is once again lower for the Crofer 22 H than for Crofer 22 APU. The images reveal good metallic contact not only at this interfacial region, but also between the anode substrate and the Ni mesh. It is important to note that these SEM images are obtained from regions where contact was achieved due to the mechanical weights subjected to the samples. Moreover, a very thin oxide layer (Cr_2O_3 + Mn-Cr spinel) is also visible, mainly on the surface of the steel plates (approx. 5 µm thick for both Crofer 22 H and Crofer 22 APU) which are outside the physical metallic contact regions but also sporadically at the interfacial zone or contact surface between the steel and the Ni mesh. In the case of the Crofer 22 H, internal oxidation within the mesh and in the case of Crofer 22 APU, oxide layers on the surface of the Ni mesh is prominent. Since Nickel diffuses faster into the Crofer22APU, it is likely that the elemental composition of the Ni mesh which is in contact with the steel plate is also altered. This may cause higher corrosion of the mesh and the formation of a chromia scale on the Ni mesh surface. The presence of an oxide layer (approx. 3 µm thick) between the Ni mesh and the anode substrate for the Crofer 22 APU from Figure 10 might explain the slightly larger ASR for these samples. However, the resistivity measurements suggest that metallic conduction dominates the electrical behavior and the formation of oxide layers is not substantially determining the properties as confirmed by the low ASR values.

Downloaded on 2014-01-13 to IP 134.94.122.141 address. Redistribution subject to ECS license or copyright; see ecsdl.org/site/terms_use

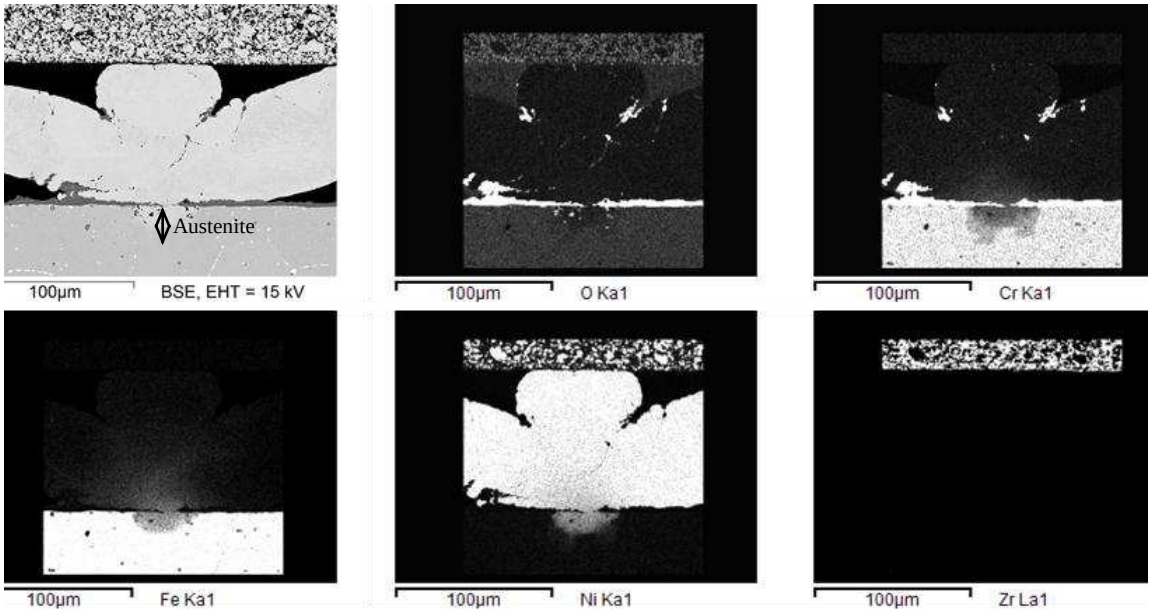

Figure 11. SEM image (upper left) and x-ray element mappings of the interfacial cross sections after 3000 hours of Crofer 22 H Steel, Ni-YSZ Cermet and Ni mesh sandwich subjected to 0.7 A.cm^{-2}. Respective elements and x-ray lines used (Kα or Lα) are indicated beneath the figures.

Not at every physical contact point between the mesh and the steel plates inter-diffusion processes were observed. This is illustrated in Figure 12. The gap visible between the mesh and the anode substrate is an artifact of sample preparation. It can be seen that in spite of the flat contour of the mesh and its compression, there are no signs of inter-diffusion at certain regions as indicated by the presence of oxide layers. Hence there exist different situations at the interface within the same sample type depending on the nature of contact and the oxygen partial pressure prevailing locally. The measured contact resistance is likely to be equal to the effective resistance of a network of parallel resistors, each of which represent different resistances of varying levels of metallic contact and formation of oxide layers.

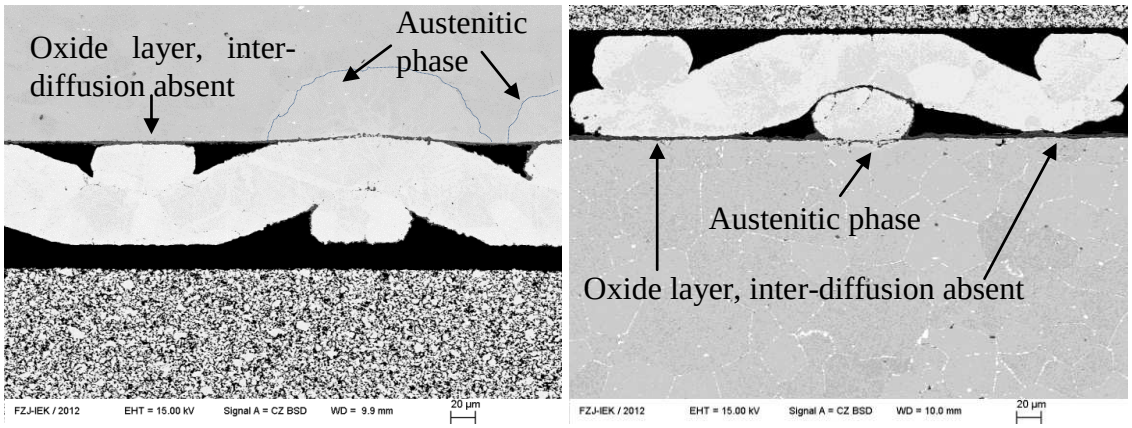

(a) (b)

Figure 12. SEM images of the interfacial cross sections after 3000 hours of (a) Crofer 22 APU Steel, Ni-YSZ Cermet and Ni mesh sandwich subjected to 0.7 A.cm^{-2} and (b) Crofer 22 H Steel, Ni-YSZ Cermet and Ni mesh sandwich subjected to no current density

Downloaded on 2014-01-13 to IP 134.94.122.141 address. Redistribution subject to ECS license or copyright; see ecsdl.org/site/terms_use

Summary and Conclusion

- Penetration/diffusion of nickel into the steel as well as Cr and Fe into the Ni-mesh leads to partial austenitization of the ferritic steels and to the internal and external oxidation of the Ni mesh. This is likely to alter the selective oxidation properties of the steel plates but might also affect their mechanical properties.
- Nickel diffuses into the steel up to a depth of 45-80 µm during 3000 h exposure in Ar + 4%H_2 + 2%H_2O at 800 °C.
- The microstructural analysis of the steel and Ni mesh sandwich samples reveal that no σ-phase is present near the contact area between the Ni-mesh and both steels Crofer 22 APU and Crofer 22 H after exposure of 3000 hours at 800 °C.
- The kinetics of inter-diffusion reveal that nickel diffuses faster into Crofer 22 APU than in Crofer 22 H
- The measured ASR under 97% H_2 + 3% H_2O across a sandwich of steel – Ni-mesh – Ni-YSZ – Ni-mesh – steel is stable for Crofer 22 H over a period of 3000 h, whereas a slightly increasing ASR starting at about 1500 h is observed for Crofer 22 APU
- The ASR or contact resistances are low and increase only slightly at higher temperatures (i.e., 800 °C). In spite of the oxidation of the nickel mesh, there remain or exist several other contact points that offer sufficient metallic conduction.
- These physical contact points also varied with the degree of interdiffusion, thickness of oxide layers because of the nature of applied mechanical pressure.
- At the measured operating conditions, the influence of the different depths of the inter-diffusion zones, the extent of internal and external oxidation of the Ni meshes and the thickness of the oxide scales on the surface of steel could not be established on the contact resistances.

Acknowledgments

The authors wish to thank all partners in the SOFC-Life project for their support and cooperation. 'The research presented in this paper has received funding within the framework of the EU project ‘SOFC-Life’ (EU FP7/2007-2013, Fuel Cell and Hydrogen Joint Undertaking FCH-JU, project No. 256’885).'

References

1. www.sofc-life.eu
2. J. Froitzheim, L. Niewolak, M. Brandner, L. Singheiser, and W. J. Quadakkers, J. Fuel Cell Science and Technology, **7**, 031020 (2010)
3. K. Hilpert, W. J. Quadakkers, and L. Singheiser, “Interconnects.” Handbook of Fuel Cells, Volume 4, John Wiley & Sons Ltd., p. 1037 – 1054, (2003)
4. W.J. Quadakkers, J. Piron-Abellan, V. Shemet, and L. Singheiser, in Metallic Interconnects for Solid Oxide Fuel Cells - a Review, Materials at High Temperatures, **20(2)**, p. 115-127 (2003)
5. G. V. V. Voort, in Embrittlement of steels, ASM International, Metals Handbook. Tenth Edition. 1: 689-736, (1990)

Downloaded on 2014-01-13 to IP 134.94.122.141 address. Redistribution subject to ECS license or copyright; see ecsdl.org/site/terms_use